GEOPHYSICS, VOL. 70, NO. 4 (JULY-AUGUST 2005); P. G101–G107, 9 FIGS.
10.1190/1.1993727

3D electrical imaging of an archaeological site using electrical and electromagnetic methods

Ana Osella[1], Matías de la Vega[1], and Eugenia Lascano[1]

ABSTRACT

Floridablanca is an 18th century archaeological site located in southern Argentina. Archaeological investigations at the site began in 1998, and in 2000 we started a project to perform geophysical studies there. In this paper, we report the implementation of electrical and electromagnetic (EM) methods in a sector of the site that corresponds to the settlers' houses. The objective of the project was to characterize the zone and the buried archaeological structures (adobe walls, tiles from a collapsed roof) with 2D and 3D electrical and EM techniques. We first applied an EM induction method covering a 600-m^2 area with a frequency ranging from 1000 to 19 000 Hz. A 3D visualization of the in-phase and quadrature components gave an initial description of anomalies possibly associated with buried structures. We then performed dipole-dipole profiles and inverted the data to obtain the corresponding 2D and 3D electrical images. Finally, after correlating the information obtained from the analysis of both EM and electrical data, we performed a more localized 3D dipole-dipole mesh (25 m^2) to achieve the final electrical image of the most representative buried structure. The combination of both techniques allowed us to map two entire houses and to identify three types of walls: main, separating, and inner. These results have been confirmed by an archaeological excavation.

INTRODUCTION

Geophysical methods are widely used in archaeology for detecting, mapping, and studying the characteristics of various types of objects and structures in the subsurface. These methods allow for evaluation of their conservation state and identification of different construction phases and areas disturbed by agricultural activities or plundering. Also, the investigation of geologic deposits and buried landforms is useful for generating paleoenvironmental information (e.g., Dalan et al., 1992; Bewley et al., 1996; Herbich et al., 1997; Silliman et al., 2000; Weston, 2001). Although these methods have been applied systematically in archaeology during the last 50 years, their implementation in Argentina is relatively new. Application of these methods in Argentina began in the mid-1990s and has been oriented mainly toward detecting buried structures from a few geoelectrical soundings (Carrara, 1996; Ponti et al., 1996).

In 2000, we began a multidisciplinary project to characterize an archaeological site in southern Patagonia. A geophysical study was carried out, including the application of electrical and EM methods, to obtain an electrical image of the subsoil.

The Floridablanca archaeological site (Figure 1) is located in San Julián Bay, Santa Cruz Province, Argentina (49° 16′38″S, 67°51′22″W). It corresponds to a little village established in the 18th century as part of a Spanish government project for the colonization and defense of the Patagonian Atlantic coast. According to historical data, a wooden fort, 50 m long and 50 m wide and surrounded by a moat, was built first (CS II, Figure 2a). People dwelt in this square fort until houses were built outside the fort. Once the settlement was enlarged with the construction of new exterior buildings, the population was redistributed. The settlement, which finally covered an area of 40 000 m^2, was abandoned after four years because of a royal order from Spain (Senatore, 2000; Senatore et al., 2001).

The geophysical research was proposed to create a map of the site (buried at present) that would show the distribution and characteristics of the underground structures. We based our work on the historical map of the site, which was complemented with data from archaeological surveys carried out since 1998 (Senatore, 2000).

Previous exploratory excavations were done in both the North Wing I and South Wing II sectors (NW I and SW II, respectively; Figure 2). Only one house was excavated in each

Manuscript received by the Editor March 4, 2004; revised manuscript received September 28, 2004; published online July 7, 2005.
[1]Universidad de Buenos Aires, Dto. de Física, Facultad de Ciencias Exactas y Naturales, Ciudad Universitaria, Pab. 1, 1428 Buenos Aires, Argentina. Also at Conicet (Consejo Nacional de Investigaciones Científicas y Técnicas), Buenos Aires, Argentina. E-mail: osella@df.uba.ar; matias@df.uba.ar; eugenia@df.uba.ar.

wing. According to historical information, these wings should correspond to settlers' houses, but there is no information about the internal organization of the houses. The house excavated in the NW I sector had no remains of the roof and exhibited a low artifact density. In the SW II sector, a collapsed roof (tiles and remains of the wooden beam) was found on the floor of the structure.

The first geophysical study focused on the NW I sector (see Figure 2). We applied ground-penetrating radar (GPR) and resistivity methods to characterize the structures and used the electromagnetic induction (EMI) method to obtain more information about the internal layers. Analysis of the data revealed a number of anomalies which, after correlation with the archaeological excavations, could be associated with adobes or similar raw-material walls. These anomalies appeared as a periodicity, which indicated that the NW I sector corresponded to a main structure divided into substructures (houses), each separated by narrower internal walls. The data gathered at the NW I sector were quite different from the data obtained in the SW II sector, where a collapsed roof was found. This result made it possible for us to conclude that the North Wing was not finished, confirming one of the main hypotheses about this sector (Lascano et al., 2003).

As a continuation to this project, this paper presents the results obtained at the SW II sector of the settlement, which should correspond to inhabited houses (Figure 2). In this case, we did not perform GPR studies because of the thick vegetation covering the area. For that reason, to obtain a first insight about the characteristics of the subsoil and to detect anomalies that could be associated with buried structures or artifacts, we decided to apply the EMI method, which does not require contact with the ground. We then selected locations to perform dipole-dipole profiles according to the EMI results. These data were inverted to obtain 2D electrical images. By combining the complete set of data, a 3D inversion was performed. Finally, using this result, we selected an appropriate place to perform a high-resolution 3D mesh. The 3D electrical image obtained from these data was used to optimize the exploratory excavation plan to locate the position of the walls delimiting the structure and to confirm the existence of roof collapses through a characterization of tile deposits.

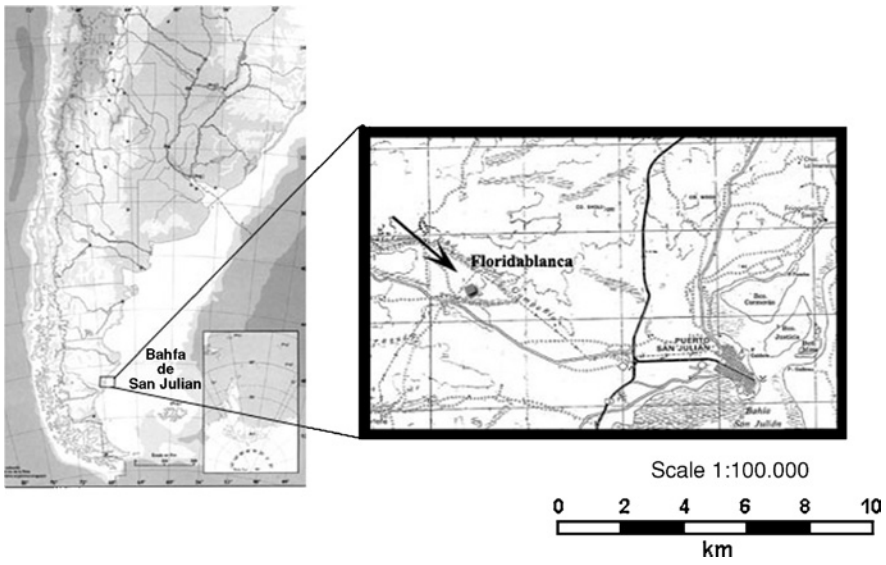

Figure 1. Location of the Floridablanca archaeological site.

DATA ACQUISITION

We studied an area of approximately 600 m^2 corresponding to the SW II sector (Figure 2). Our aim was to look for evidence of buried structure — more precisely, adobe walls — to delimit these structures and to study the presence or absence of ceramic tiles from a collapsed roof within the sector under study. To do so, we applied both electrical and EMI methods.

To acquire the EM data, we used a GEM-300 multifrequency EM profiler (Won et al., 1998). This system consists mainly of two small coils — a transmitter and a receiver — separated by a constant distance of 1.67 m and moved along a profile. The secondary field detected at the receiver is separated into in-phase I and quadrature Q components expressed in parts per million against the primary field. The profiler has a frequency range from 300 to 19 975 Hz, allowing for a maximum of 16 survey frequencies.

The electrical surveys were done using the Saris 500 multielectrode resistivimeter. We deployed dipole-dipole arrays; to create electrical images, we inverted the 2D profiles using the DCIP2D inversion code developed by the University of British Columbia (UBC) in 2001,

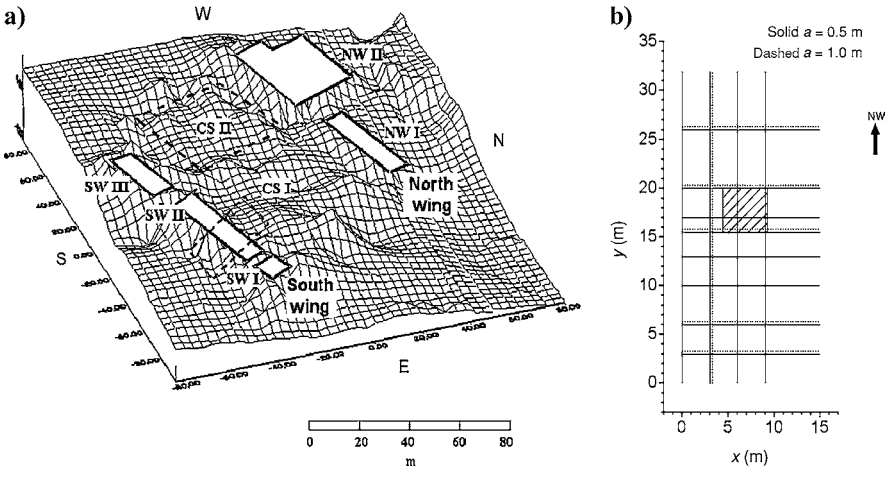

Figure 2. (a) Map of the site and its subareas. Local topography defined the different sectors. The rectangle across the SW II sector indicates the area being surveyed. (b) Locations of the 2D dipole-dipole profiles across the study area marked in Figure 2a. The dotted square indicates the 3D mesh.

based on the work of Oldenburg et al. (1993) and Oldenburg and Li (1994). We also performed 3D inversions using a DCIP3D inversion code created in 2003.

ELECTROMAGNETIC DATA

The EMI profiles were performed along the *y*-direction (Figure 2b). Both the inline and broadside surveys (instrument direction parallel and perpendicular, respectively, in the direction of survey lines) were carried out, with the dipole direction parallel and perpendicular to the ground. This was done to determine the configurations giving the best resolution for this particular job. The data along the profiles were collected at increments of 1 m. Sixteen profiles were carried out with a separation of 1 m in the *x*-direction between consecutive lines, thus covering the complete area.

Because the EM signals penetrated greater depths with decreasing frequencies, we selected 16 frequencies from 1000 to 19 000 Hz to guarantee good resolution for the first layers [see, e.g., Won et al. (1998)]. After analyzing the results from the different configurations, we concluded that the best resolution was achieved when the magnetic dipole moment was parallel to the ground (as expected), since we were looking for very shallow structures [see, e.g., Witten et al. (1997)]. In Figure 3, the in-phase and quadrature components for the inline survey with magnetic dipole moments in the *x*-direction are shown for four representative frequencies. In Figure 4, the same components are displayed for the broadside survey, with magnetic dipole moments in the *y*-direction. The data are visualized as slice maps for the different frequencies.

The intensity of the response increases with the conductivity of the medium and decreases with depth (i.e., with decreasing frequency). Therefore, we can draw some conclusions from the distribution of the quadrature component (Figure 3b). The greater response region (from approximately $y = 25$ m up to the end of the area) corresponds to the square of the village (CS I, Figure 2a), while the first 20 m include the zone where the houses are believed to be buried, taking into account the differences in vegetation. This contrast is observed for the highest frequencies; but as frequencies decrease, which implies deeper imaging, the distribution becomes more homogeneous. For the lowest frequencies, the differences are even smaller.

The most interesting features can be observed between $y = 10$ m and $y = 25$ m, marked as ovals in Figure 3b. The lowest responses may be attributable to the presence of tiles, which may be scattered between the house walls if a roof collapse really occurred, as historical chronicles indicate. A possible explanation is that these materials have a greater contrast with the surrounding medium, thus appearing in the data as a negative anomaly [an absence of conductivity; see Witten et al. (2003)]. If this is the case, this low-response distribution may not only indicate the presence of tiles but also the location of the internal walls of the houses, appearing as discontinuities in this anomaly. This behavior is repeated in Figure 4b, which corresponds to the broadside survey (magnetic moment along the *y*-direction).

The in-phase component, on the other hand, does not present strong anomalies. The response of this component depends on both the electrical conductivity and the magnetic permeability and is particularly sensitive to highly conductive materials. That is why this component is referred to as the metal detector mode (Won et al., 1998). In this particular case, the values are relatively low (Figures 3a and 4a, respectively), suggesting the absence of metal artifacts.

Summing up, given the results from the EMI data, the presence of structures can be inferred between $y = 10$ m and $y = 20$ m; we can also detect a certain alignment of these structures along the *x*-direction. Also, there is a possibility of another structure in a perpendicular direction between $x = 0$ and $x = 8$ m (Figures 3b and 4b). To confirm these results and also to have a quantitative characterization of the structures, we performed electrical profiles along lines parallel and perpendicular to the direction of alignment.

2D ELECTRICAL TOMOGRAPHIES FROM DIPOLE-DIPOLE DATA

Taking into account the results obtained from the EMI data, we performed 2D dipole-dipole profiles along both the *x*- and *y*-axes. We carried out eight profiles along the *x*-direction, aligned with the anomalies, and four profiles perpendicular to them (see Figure 2). To obtain a good lateral resolution as well

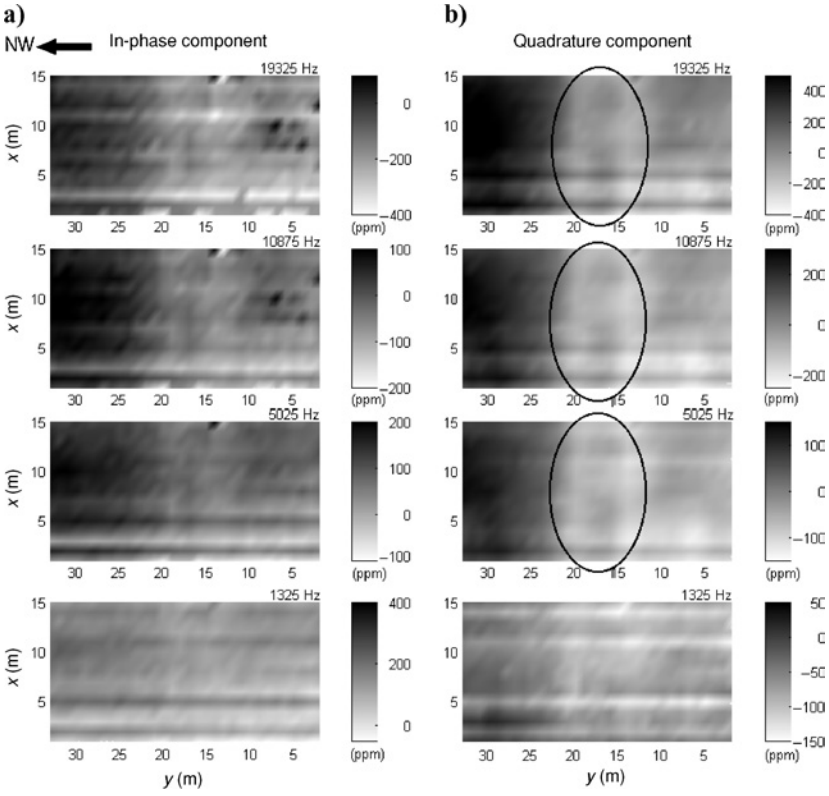

Figure 3. (a) In-phase and (b) quadrature components, in parts per million, for four frequencies corresponding to inline surveys with magnetic moments along the *x*-direction. The ovals indicate the location of the resistive anomalies.

as large penetration, electrode separations of 0.5 and 1 m were combined.

As stated previously, we inverted data using the DCIP2D inversion code. This program requires control parameters whose values are modified to obtain a good convergence. The best results were achieved using the recommended default values. In Figure 5, electrical images obtained by inverting the data are shown for profiles parallel to the x-direction. We selected a view angle that allowed the best visualization for all profiles. To perform the inversion, the topography shown in Figure 2 was included.

The topography shows the presence of a mound along the x-direction between approximately $y = 10$ m and $y = 20$ m, below which archaeological structures should be found, as inferred from the results of the EMI data. The profiles located over the mound ($y = 13$, 15.5, and 17 m, respectively) have a resistive behavior, with resistivity values higher than those obtained for the profiles located over the downgoing slopes (at $y = 10$ and 20 m). The profiles located outside the mound (at $y = 0$ and 26 m) present the lowest resistivity values. Thus, there is a completely different behavior under the elevation that defines the SW II sector and the remaining area. In previous work (Lascano et al., 2003), a preliminary study was conducted to estimate the electrical resistivity values for the walls and tiles. According to those results, the highest values of resistivity found in the profiles over the mound can be associated with the presence of tiles, and the lower values for these profiles can be associated with the walls that delimit the houses (solid lines in Figure 5). Between these walls, a slight decrease in the resistivity can be seen, which can be the manifestation of the presence of narrower inner separating walls (dashed lines in Figure 5). An important result is the separation of 6 m between the walls, which, according to the historical map, should correspond to the width of each house. The inner walls, on the other hand, should divide the houses into two rooms.

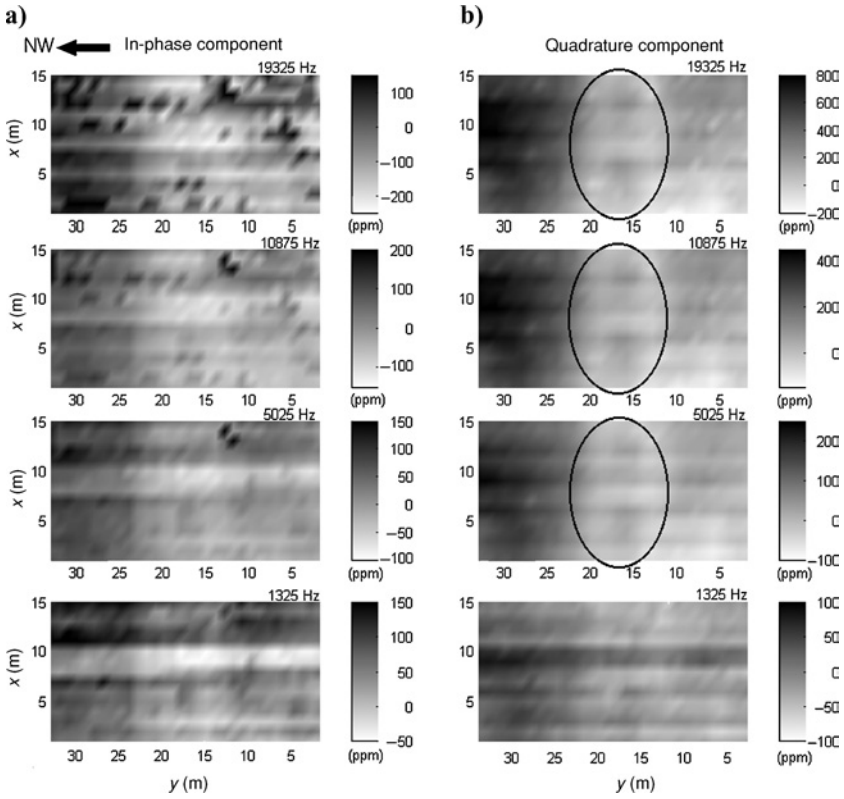

Figure 4. (a) In-phase and (b) quadrature components, in parts per million, for four frequencies corresponding to broadband surveys with magnetic moments along the y-direction. The ovals indicate the location of the resistive anomalies.

A different behavior is observed in the two profiles located over the slopes of the mound ($y = 10$ and 20 m). The resistivity distribution of the last profile is more uniform and becomes more conductive as it approaches the square ($y = 26$ m). On the other side of the mound, some high-resistivity features are still detected, even in the profile located at $y = 0$ m. This may indicate a continuity of the underground structure outside the mound in the y-direction, at least for the profile corresponding to $y = 10$ m, according to the EMI results (Figures 3b and 4b).

We also performed resistivity profiles along the y-direction. Electrical images along these profiles are shown in Figure 6 (all profiles are corrected for topography). The profiles located at $x = 3$, 6, and 9 m, respectively, show the resistive signature associated with tiles. The location of two walls can also be detected (solid lines, Figure 6)— in this case, the main walls of the houses. This feature is not repeated in the profile at $x = 0$ m, but we can see that the resistivity values are similar to the ones associated with the walls.

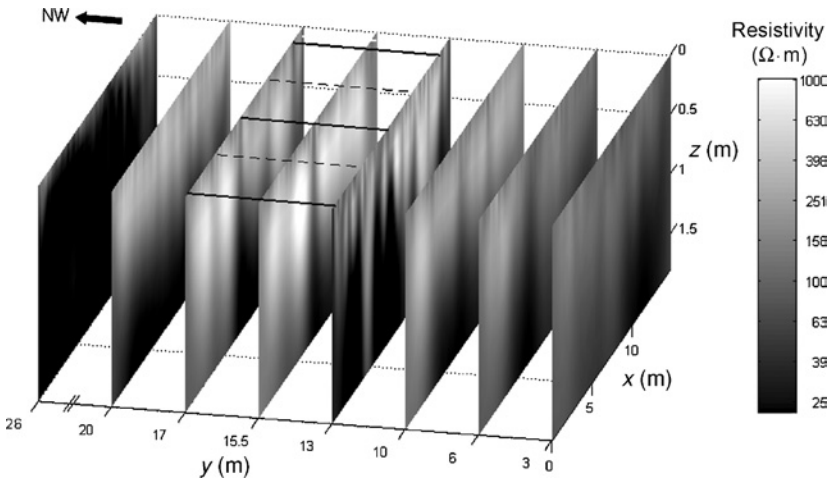

Figure 5. Electrical images corresponding to dipole-dipole profiles along the x-direction. Solid lines indicate the probable location of the separation walls; dotted lines correspond to the internal walls.

We assume that this profile was carried out precisely over one of the walls. Note the different behaviors at the ends of the profiles. The resistivity decreases toward the square but remains high toward the other side, supporting the assumption that the underground structure continues outside the mound.

3D ELECTRICAL IMAGING

The data analyzed in the previous section were also used to perform a 3D study. Although the profiles do not form a dense grid, this analysis has the advantage of correlating the data as a whole, including dipole-dipole profiles along both x- and y-directions. We assumed the profiles along the x-direction were spaced evenly between $y = 3$ and 20 m (see Figure 2b). The profile at 26 m was assumed to be representative of the zone between 20 and 32 m because this zone, which corresponds to the square, is rather homogeneous (as seen from EMI results, Figures 3 and 4, respectively). On the other hand, the profiles along the y-direction are well spaced for the region between $x = 0$ and 9 m. Summing up, we expected a reliable result of the inversion in the region bounded by $x = 0$ and 9 m and by $y = 3$ and 26 m.

These data were inverted using the DCIP3D code, including topographic corrections (Figure 2). The mesh was designed taking into account the heterogeneous distribution of electrodes. Figure 7 shows the results corresponding to a depth of 0.5 m. The dashed lines indicate the location of the structures. Along the y-direction, this anomalous zone is completely situated in the reliable part of the inversion. In the x-direction, this result is well resolved up to $x = 9$ m. We considered this anomaly to be a structure. It is limited by well-aligned regions (walls) with values of resistivity similar to the ones found previously (about 150 $\Omega \cdot$ m) enclosing a high-resistivity zone (800–1000 $\Omega \cdot$ m) associated with tile deposits. In the middle of this structure, at $x = 7$ m, is a straight structure along the y-direction, interpreted to be the internal wall separating two settlers' houses, as detected from the 2D tomographies (Figures 5 and 6). The region toward the square, between $y = 25$ and 32 m, is homogeneous, and no structures are present. On the other hand, a highly resistive anomaly (about 800 $\Omega \cdot$ m) appears in the region between $y = 5$ and 12 m and $x = 0$ and 5 m. This anomaly may indicate the presence of tiles spread outside the main houses or even some kind of lateral structure not yet well defined. These features are clearly seen up to a depth of 0.60 m; below that, they are not detected.

One of the goals of our study was to determine a site for an excavation. This site should include a room in order to differentiate between the diverse types of walls and confirm the existence of a collapsed roof, which should imply that the house had been occupied. The selected area (white arrow, Figure 7) had a high probability of containing part of the settlers' houses, and we assumed we would achieve high-resolution electrical imaging of a representative buried structure. To properly evaluate the area, we performed a 3D dipole-dipole mesh (20 dipole-dipole profiles, 10 in each direction), covering 25 m^2, as shown in Figure 2. The electrode separation was 0.5 m to ensure good lateral resolution, and topography corrections were performed when inverting the data.

The results are shown in Figure 8, where some representative planes are selected. For the shallowest plane the distribution is irregular because of the features of the terrain. At a depth of approximately 0.3 m, the locations of two walls are clearly mapped (resistivity values about 120–140 $\Omega \cdot$ m). The wall that should correspond to a main wall was wider (approximately 0.8 m) and was located at approximately $y =$ 18 m, in accordance with the global 3D image. The other wall, perpendicular to it, is narrower (about 0.3 m) and confirms a separating wall. The tile deposits (resistivity about 800 $\Omega \cdot$ m)

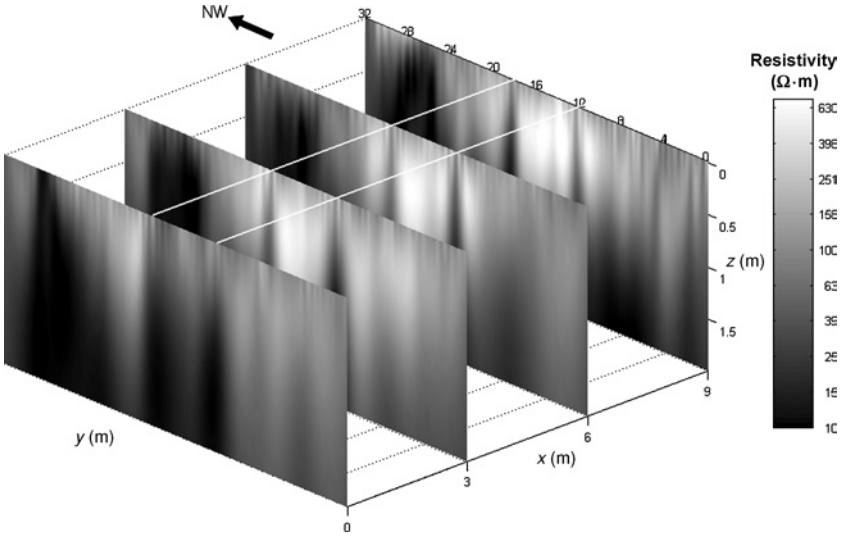

Figure 6. Electrical images corresponding to dipole-dipole profiles along the y-direction. Solid lines indicate the probable location of the main walls of the houses.

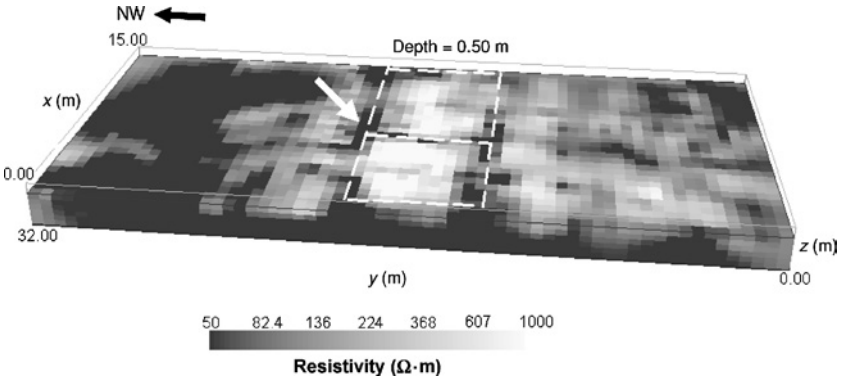

Figure 7. Three-dimensional electrical imaging obtained from the inversion of the complete set of electrical data. The dashed lines show the boundaries of two houses. The white arrow indicates the zone where a dense 3D mesh was carried out.

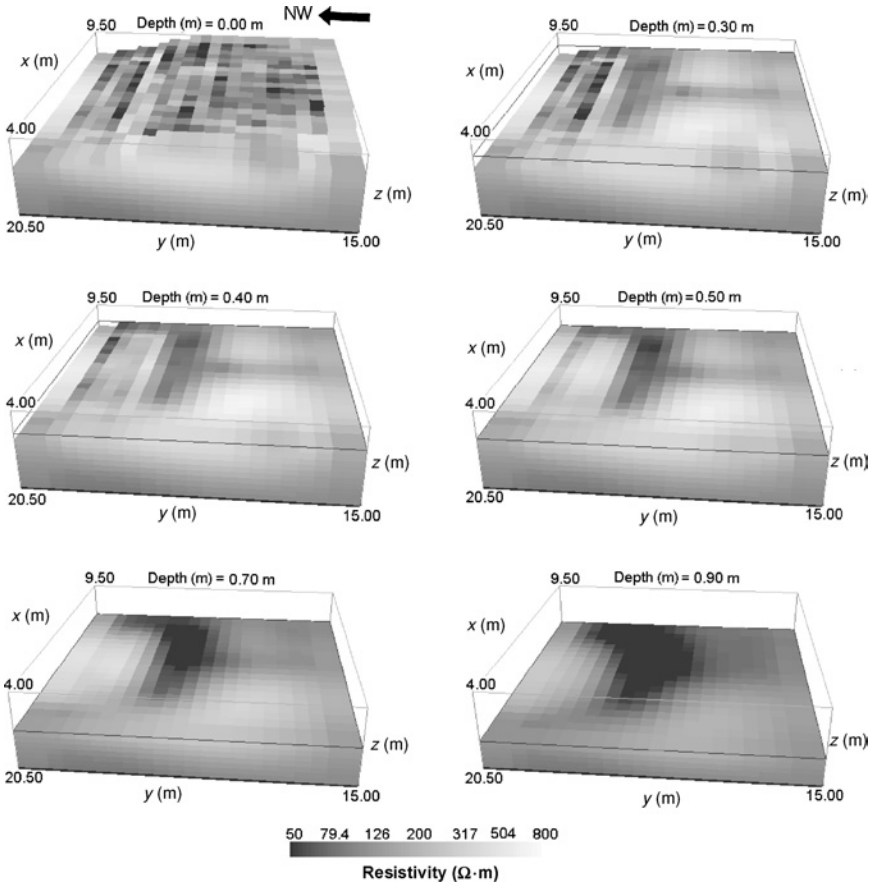

Figure 8. Three-dimensional electrical imaging corrected by topography. The main and separating walls of one of the houses are clearly seen from 0.30 to 0.60 m. The most resistive material corresponds to tile deposits.

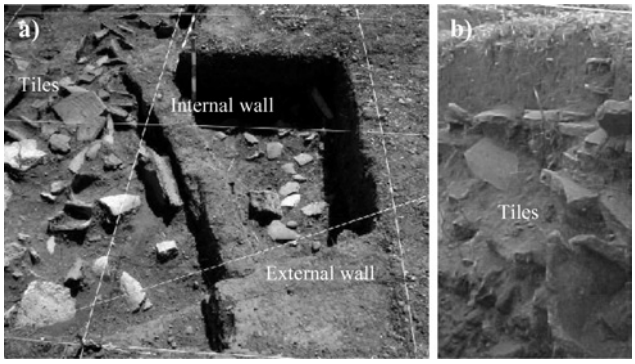

Figure 9. (a) View of the sector excavated using the 3D electrical imaging shown in Figure 8. Details of the separating wall and evidence of the main wall can be observed. Also, the presence of tiles between the walls is confirmed. (b) View of the tile deposit. According to the scale shown in the photo, the thickness of the deposit is approximately 40 cm.

can also be seen. This image is repeated down to approximately 0.7 m. At this depth, the resistivity begins to decrease to values of 50 $\Omega \cdot$m, which is characteristic of the subsoil, mainly formed by clays. One can conclude that the height of the walls is no more than 0.4 m. The fact that the walls had not been completely covered during the years and thus part of them had been destroyed must be taken into account. That is why a small part of the wall still remains at a shallow depth.

A recent excavation has exposed these walls. Figure 9a is a picture of the exposed structures, confirming the presence of a heterogeneous layer of tiles nearly 0.40 m thick (Figure 9b).

CONCLUSIONS

For the first time in Argentina, archaeogeophysical prospecting including 3D electrical imaging has been successfully performed to map an 18th-century Spanish village in Patagonia. We applied the EMI method to detect and locate anomalous zones that could be associated with buried anthropologic structures. Then, according to these results, we deployed dipole-dipole profiles to obtain 2D and 3D high-resolution images.

As an initial approach, the EMI method proved to be a good option, compared to GPR techniques, for locating anomalies when dealing with an irregular area. Although both methods provide efficient coverage of large areas, the main advantage of EMI is that it can be applied regardless of contact with the ground. Covering the complete area took us one day of field work and another day of visualizing the data and locating the anomalies. The results allowed us to define an optimal strategy for the high-resolution study.

The electrical images obtained from 2D and 3D inversions of the dipole-dipole data provided high-resolution lateral results and good in-depth localization when combining different electrode apertures. Although electrical imaging cannot be compared with EMI in terms of time needed to cover an extensive area, it is the best method for high-resolution imaging when anomalous zones have been detected.

Using the results from 2D and 3D imagings, we mapped two entire houses. We could discriminate three types of walls: main walls of the whole structure, separating walls between adjacent houses, and internal walls within the houses. Their widths were approximately 0.8, 0.4, and 0.2 m, respectively. All of the walls were found at a depth of 0.30 m and were 0.40 m high. Inside the houses, the presence of tiles confirmed a collapsed roof. These tiles formed a 0.40-m-thick layer, which is why they were detected with both EMI and geoelectrical data. Otherwise, isolated tiles would not have produced a detectable anomaly. This collapsed roof also indicates that the houses in this sector were inhabited. These results were used to define an area for an exploratory archaeological excavation. The materials exposed by the dig verify the quantitative results with remarkable accuracy.

The combination of these techniques allowed us to map a sector of the site accurately and contributed to a more precise plan for the archaeological excavations. We also achieved a quantitative description of the geometric characteristics and

location of the walls. The map constructed for the site made it unnecessary to perform a complete excavation of the area, thus preserving its archaeological value.

ACKNOWLEDGMENTS

This work was supported in part by Agencia Nacional de Promoción Científica y Tecnológica (National Agency for Scientific and Technological Promotion). We thank Area Geofísica Engineering for allowing us to use its GEM-300 equipment. We also thank the archaeological team, especially M. X. Senatore and S. Buscaglia.

REFERENCES

Bewley, R., M. Cole, A. David, R. Featherstone, A. Payne, and F. Small, 1996, New features within the hedge at Avebury, Wiltshire: Aerial and geophysical evidence: Antiquity, **70**, 639–646.

Carrara, M. T., 1996, Santa Fe La Vieja, first settlement in the Parana region (in Spanish): Journal of Anthropology of the Rio de la Plata Region, **2**, 135–146.

Dalan, R. A., J. M. Musser Jr., and J. K. Stein, 1992, Geophysical exploration of the shell midden in deciphering a shell midden: Academic Press.

Herbich, T., K. Misiewicz, and O. Teschauer, 1997, Multilevel resistivity prospecting of architectural remains: The Schwarzach case study: Archaeological Prospection, **4**, 105–112.

Lascano, E., A. Osella, M. de la Vega, S. Buscaglia, X. Senatore, and J. L. Lanata, 2003, Geophysical prospection at Floridablanca archaeological site, San Julián Bay, Argentina: Archaeological Prospection, **10**, 1–18.

Oldenburg, D. W., and Y. Li, 1994, Inversion of induced polarization data: Geophysics, **59**, 1327–1341.

Oldenburg, D. W., P. R. McGillivary, and R. G. Ellis, 1993, Generalized subspace method for large-scale inverse problems: Geophysical Journal International, **114**, 12–20.

Ponti, N., G. Fanton, A. Imhof, and S. Pastore, 1996, Archaeological investigations at Santa Fe La Vieja, Santa Cruz Province, Argentina (in Spanish): Journal of Anthropology of the Rio de la Plata Region, **2**, 128–130.

Senatore, M. X., 2000, Archaeology of Floridablanca, Santa Cruz Province (in Spanish): Annals of the National Academy of Science, Buenos Aires, **34**, 743–753.

Senatore, M. X., M. Bianchi Villelli, S. Buscaglia, and M. Marschoff, 2001, Archaeological map of the Floridablanca Spanish fort, San Julián, Argentina: Relaciones, **36**, 323–344.

Silliman, S. W., P. Farnsworth, and K. G. Lightfoot, 2000, Magnetometer prospecting in historical archaeology: Evaluating survey options at 19th-century Rancho site in California: Historical Archaeology, **34**, 89–109.

Weston, D. G., 2001, Alluvium and geophysical prospection: Archaeological Prospection, **8**, 265–272.

Witten, A., I. J. Won, and S. Norton, 1997, Imaging underground structures using broadband electromagnetic induction: Journal of Environmental and Engineering Geophysics, **2**, 105–114.

Witten, A., G. Calvert, B. Witten, and T. Levy, 2003, Magnetic and electromagnetic induction studies at archaeological sites in southwestern Jordan: Journal of Environmental and Engineering Geophysics, **8**, 209–215.

Won, I. J., D. Keiswetter, and E. Novikova, 1998, Electromagnetic induction spectroscopy: Journal of Environmental and Engineering Geophysics, **3**, 27–40.